

Short Report

From Low Cost UAV Survey to High Resolution Topographic Data: Developing our Understanding of a Medieval Outport of Bruges

JEROEN DE REU^{1*}, JAN TRACHET¹, PIETER LALOO² AND WIM DE CLERCQ¹

¹ Department of Archaeology, Ghent University, Sint-Pietersnieuwstraat 35, B-9000 Ghent, Belgium

² GATE bvba, Eindeken 18, B-9940 Evergem, Belgium

ABSTRACT This paper assesses the application of a consumer-grade unmanned aerial vehicle (UAV) solution for the image-based three-dimensional (3D) reconstruction of a buried Medieval landscape at Monnikerede, a deserted former outport of Bruges, with the archaeological aim to achieve a better characterization of the (micro)topography and ultimately a better understanding of the site. The UAV survey resulted in a highly detailed and accurate 3D model of the terrain, allowing a thorough topographic analysis of the complex archaeological landscape. Application of algorithms to produce an enhanced visualization of the topographic variability led to a sequence of derivatives each highlighting the topography in a different way. Additionally a decorrelation stretch was applied on the collected imagery, thereby generating enhanced orthophotos producing another DSM view on the archaeological landscape. Integrating the (enhanced) orthophoto(s) with the digital surface model (DSM) and derivatives to conduct a thorough analysis of the archaeological landscape resulted in the detection and identification of new archaeological features and the formulation of new insights in the layout of this important Medieval outport. Copyright © 2016 John Wiley & Sons, Ltd.

Key words: UAV; image-based 3D reconstruction; structure from motion; DSM; topographic analysis; orthophoto; decorrelation stretch; Belgium

Introduction

During the Middle Ages, the city of Bruges became a leading cultural and economic centre in Europe. The linear gateway that connected the town's commercial centre with the North Sea played a crucial role in this development. From the twelfth century onwards, the natural tidal inlet of the *Zwin* was gradually adapted for seaborne trade through the construction of dikes, sluices and smaller ports of transshipment. One of these port sites is the deserted settlement of

Monnikerede. During the mid-nineteenth century, Janssen (1854) observed complex (micro)topographic features and remains of Medieval land use at the assumed location of the disappeared outport. Until today, the interpretation of these topographic features remained unclear and in need of discussion (e.g. Hillewaert 1986). Aiming at a more specific characterization of the microtopography, and to achieve a better understanding of the buried archaeological landscape, we conducted an (low-cost) unmanned aerial vehicle (UAV) survey of the area.

UAVs are extensively used in modern-day society (e.g. delivery, medical applications and film industry) and research communities (e.g. Lucieer *et al.*, 2013;

* Correspondence to: Jeroen De Reu, Department of Archaeology, Ghent University, Sint-Pietersnieuwstraat 35, B-9000 Ghent, Belgium. E-mail: jeroen.dereu@ugent.be

Torres-Sánchez *et al.*, 2013; Whitehead *et al.*, 2014), and are used for image acquisition in photogrammetry and image-based three-dimensional (3D) reconstruction (e.g. Colomina and Molina, 2014; Whitehead and Hugenholtz, 2014). UAVs hold great potential for archaeology; to collect aerial images, to map archaeology or to protect and monitor endangered sites (e.g. Chiabrando *et al.*, 2011; Eisenbeiss and Sauerbier, 2011; Ortiz *et al.*, 2013; Nex and Remondino, 2014).

UAVs come in different shapes and sizes, with different payloads and user control, and at greatly different costs (Watts *et al.*, 2012). Especially costs are a boundary for the UAV to be integrated in the archaeologist's toolkit. Therefore, besides the aimed landscape characterization, it is our aim to assess the potential (and limitations) of a consumer grade, low cost UAV solution (DJI Phantom 2) for the image-based 3D reconstruction of this complex Medieval landscape.

Materials and methods

Case study: the deserted Medieval town of Monnikerede

The first attestations of the site are found in early thirteenth century English documents that speak of merchants from Monnikerede who conducted trade with their ships in the Bay of Biscay and England (De Smet, 1937). Already by then, the small landing site and fishing village of Monnikerede seems to have been integrated in the international trade network of Bruges (Figure 1). Halfway through the thirteenth century, the village was granted city rights from the Flemish count and staple rights from the city of Bruges (Gilliodts-Van Severen, 1891). For nearly two centuries, Monnikerede profited from Bruges' booming economy and transformed from a small landing site into a miniature city. However, the recession of Bruges' economy and the regression and silting of the tidal inlet, demonstrated

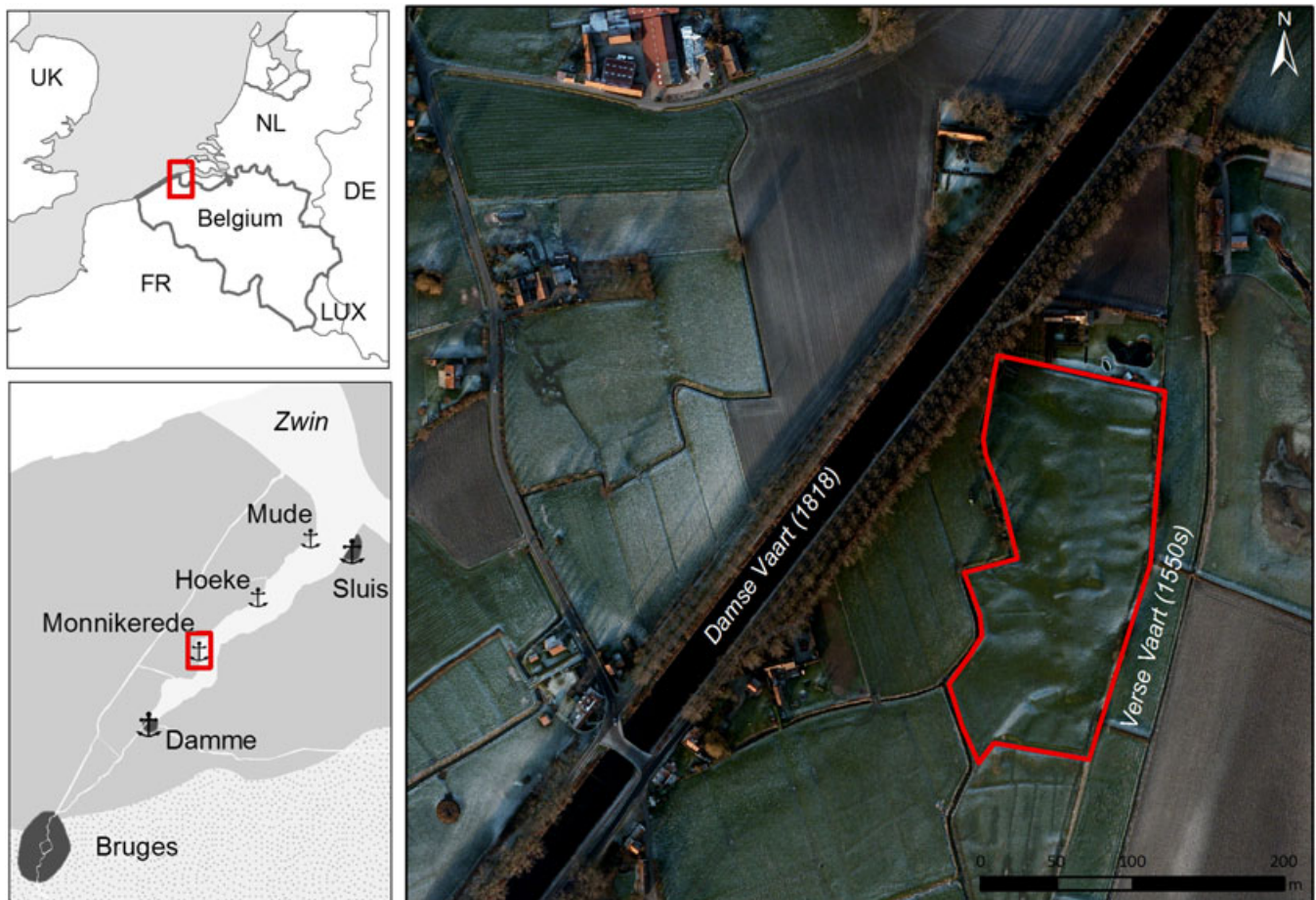


Figure 1. Location of the study area in Belgium (bottom left), in relation with Bruges and the historic Zwin (Medieval situation) (top left). The current situation is visible on a recent orthophoto (AGIV, 2008) (right). The red contour line delineates the field under study.

that Monnikerede was not viable without the network in which it existed (Sosson, 1993). In an attempt to restore the navigable connection between Bruges and the sea, the canal 'Verse Vaart' was dug (1548–1557) (Ryckaert and Vandewalle, 1982). Although the course of this new waterway was dug into the former bed of the tidal inlet, it partly intersected the former fifteenth-century city-expansion constructed outside the dike on the alluvial bed. As the construction of the canal never brought the revival and with increasing military tensions of the Spanish–Dutch war being fought in the region, Monnikerede further declined and gradually shrank into a sparsely populated hamlet (Gilliodts-Van Severen, 1891). Eventually, it officially renounced its city rights to Damme in 1594. This slow decline was accelerated by the construction of the Damse Vaart, a Napoleonic canal that cuts straight through the former centre of Monnikerede. In particular this last waterway profoundly changed the outlook of the site, dividing it in two parts, disfiguring the medieval landscape. West of the Napoleonic canal, the site transformed into arable land, while the eastern part became a pasture up until today. This meadow therefore still bears the unique topographical features of medieval habitation and exploitation (Figure 1). As the area comprises 3.5 ha (35,000 m²), archaeologists are confronted with the methodological challenge to

assess and to map the vast topographical remains, in order to add to the understanding of this substantial part of the former Medieval town.

Available topographic data

Although Janssen (1854) already described the peculiar microtopography of the western part of the site in the mid-nineteenth century, it took until 1986 before the first proper archaeological and topographical study was conducted. The research consisted of an altimetric survey of more than 2000 measurements which were interpolated into a 2.5D model of the site. Unfortunately, the raw data were lost over the years. The only remaining record is a published 0.5 m interval contour map of the terrain (Hillewaert, 1986). This contour map was digitized for interpretative and comparative means (Figure 2a). In January 1999, the site was monitored during one of the aerial surveys of the Department of Archaeology of Ghent University (Bourgeois *et al.*, 2002). A set of five photographs clearly depict the topography of the field as shadowmarks. These aerial photographs were georeferenced using the methods described by Verhoeven *et al.* (2012). The result was adequate for georeferencing the shadowmarks, but it was however of insufficient quality to be used for a topographic study (Figure 2b). In

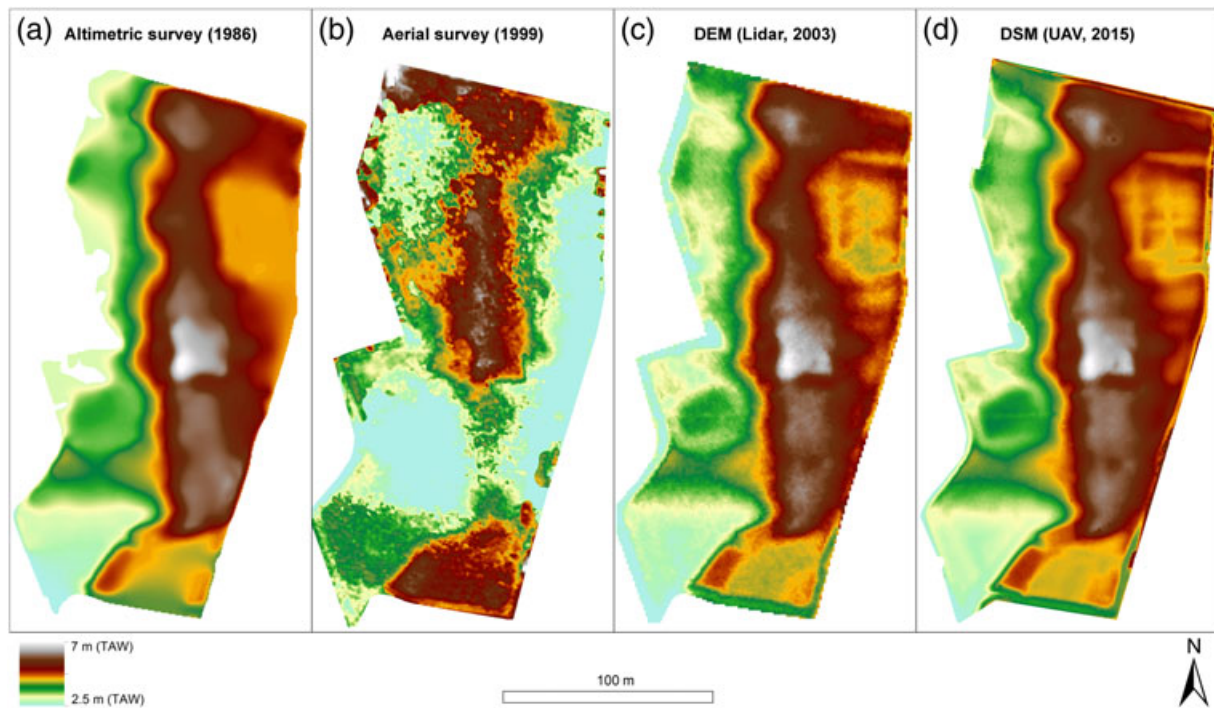


Figure 2. Comparison between the available topographic data and the digital surface model (DSM) derived from the unmanned aerial vehicle (UAV) survey.

2003, a first generation airborne LiDAR (light detection and ranging) survey, with an average point density of 1 point per 2 m² and an altimetric accuracy ranging between 7 and 20 cm, was conducted in Flanders (AGIV, 2003; Werbrouck *et al.*, 2011). From this dataset, a local digital elevation model (DEM) with 1 m resolution was generated (Figure 2c).

UAV survey

The consumer grade DJI Phantom 2 UAV, a light-weight quadcopter, equipped with a GoPro Hero 3+ (black edition) camera was applied to conduct the survey. The UAV was manually controlled, from the ground, by the pilot, resulting in a slightly irregular flight pattern and flight altitude. The average flight altitude (above the terrain) was 8.9 m. During the 24 minutes flight, the camera, with rolling shutter, was set to take one image every 0.5 seconds, resulting in a dataset of more than 2000 12MP (4000 × 3000) images. A lens correction was applied before using the images for image-based 3D reconstruction – in the newer versions of the software PhotoScan (from version 1.1 onwards), a lens correction of the fish-eye like GoPro imagery is no longer necessary. A camera calibration of the images shot by these types of non-rectilinear lenses is now performed during the structure from motion step in the image-based 3D reconstruction workflow.

The software PhotoScan (professional edition, version 1.0; Agisoft LLC, 2015) was used to generate the 3D landscape model, following the image-based 3D reconstruction workflow described by Verhoeven (2011) and De Reu *et al.* (2013b). Many researchers have already discussed the application of the software package in archaeological research and described the accuracy of 3D models obtained with it (e.g. Doneus *et al.*, 2011; De Reu *et al.*, 2013b, 2014; Koutsoudis *et al.*, 2014). 72 ground control points (GCPs), with known *x*-, *y*- and *z*-coordinates, were collected in the field using a Trimble R10 RTK-GPS with differential corrective. These GCPs were collected to be used in the bundle adjustment, to achieve an absolute georeferencing of the scene, and to make an accuracy assessment of the 3D model. Once georeferenced, an orthophoto and digital surface model (DSM) were extracted from the 3D model. The data were processed using a Dell™ Precision™ T7500 with One Intel® Xeon® X5680 (3.33 GHz, 6.4 GT/s, 12 MB, 6C) processor, 24 GB DDR3 1333 MHz ECC-RDIMM (6 × 4 GB) memory, a 64-bit operating system (Windows 7) and a 2 GB GDDR5 ATI FirePro V7800 graphic card.

Topographic analysis

A 2.5D DSM was extracted from the georeferenced 3D model to conduct a detailed study of the (micro)topographic variations on the site (Figure 2d). Several algorithms were applied to further visualize, analyse and interpret the topographic variability (Figure 3). A slope analysis was performed to calculate and visualize the slope, in percentage and degree, as well as the slope direction. A principal component analysis, as described by Devereux *et al.* (2008), was conducted using a sequence of 16 hill-shaded images (with a 22.5° variation in azimuth). The sky-view factor, or the portion of sky visible from each point in the DSM (Kokalj *et al.*, 2011; Zakšek *et al.*, 2011), was applied using various search radii. Local topographic analyses were conducted using the elevation residuals, including difference from mean elevation, standard deviation of elevation and deviation from mean elevation, described by Gallant and Wilson (2000). Difference from mean elevation measures the difference at a certain point and the average elevation around it within a predefined search radius, standard deviation of elevation measures the variability of elevation around a central point within a predefined search radius, and deviation from mean elevation measures the elevation at the central point as a fraction of the local relief normalized to local surface roughness within a predefined search radius (Gallant and Wilson, 2000; De Reu *et al.*, 2013a). The search radii applied for the local topographic analyses ranged, every 0.5 m, between 0.5 m and 10 m.

To detect minimally visible colour differences (e.g. crop marks) in the imagery, a decorrelation stretch was applied to colour enhance all individual images (Figure 4). These enhancements were conducted using DStretch, a plug-in for the open source software ImageJ (Harman, 2014). The enhanced images were mapped on top of the 3D model (instead of the regular texture mapping), resulting in an enhanced 3D model of the landscape. The application of image enhancements has already demonstrated its relevance for archaeological research. It particularly proved useful in the study and interpretation of rock art (e.g. Caldwell and Botzjorn, 2014; Cerrillo-Cuenca and Sepúlveda, 2015).

Results

Despite the slightly irregular flight pattern and flight altitude (both a result of the manual control of the UAV), we were able to generate a highly detailed

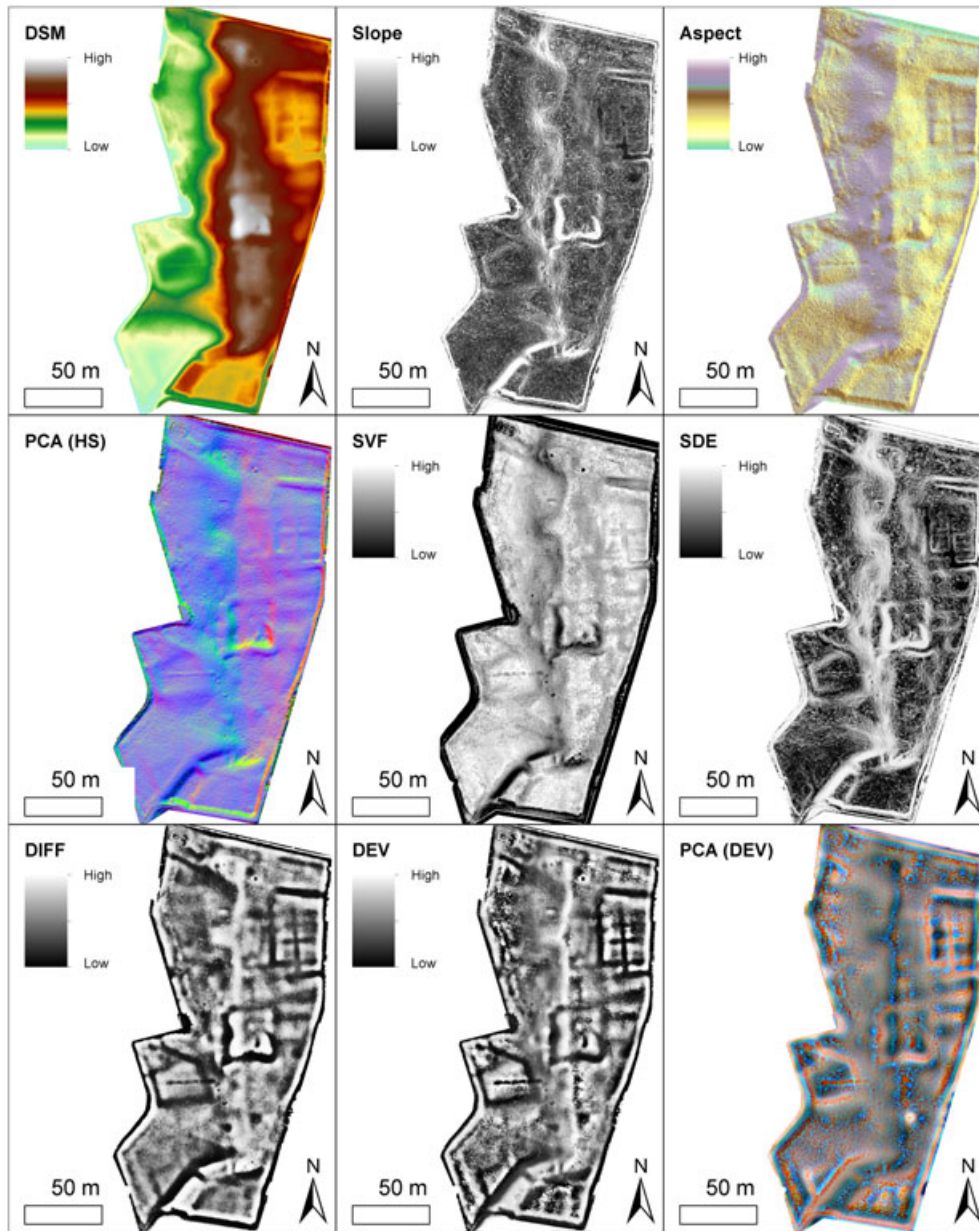


Figure 3. The DSM generated through image-based 3D reconstruction of the UAV survey imagery and its derivatives: slope (in percentage); slope orientation (aspect); principle component analysis of 16 hill-shaded images (PCA HS); sky-view factor (3 m search radius) (SVF); standard deviation of elevation (0.5 m search radius) (SDE); difference from mean elevation (5 m search radius) (DIFF); deviation from mean elevation (4 m search radius) (DEV) and principle component analysis of 20 deviation from mean elevation images (search radii from 0.5 till 10 m, with 0.5 m interval) (PCA DEV).

and accurate 3D model of the terrain. The total RMSE (root mean square error) of the model reported between the computed coordinates and the values of the 72 GCPs measures 5.2 cm and the individual RMSE for the x -, y - and z -axis measure, respectively, 2.9, 3.2 and 2.9 cm. A DSM with 2.88 cm cell size could be derived from the 3D model. The vertical accuracy of the DSM was evaluated with a sample of 739 random measurements, scattered over the terrain, and collected

with a Trimble R10 RTK-GPS with differential corrective. The standard deviation between the measured z -values, at a certain xy -location, and the z -values, at this xy -location in the 3D model is 3.6 cm. The deviance between the measured points and the DSM ranges, for 90% of the reference points between -5.88 cm and 5.75 m. The topographic model of the site obtained through the UAV survey is without doubt of a much higher resolution than the previously available

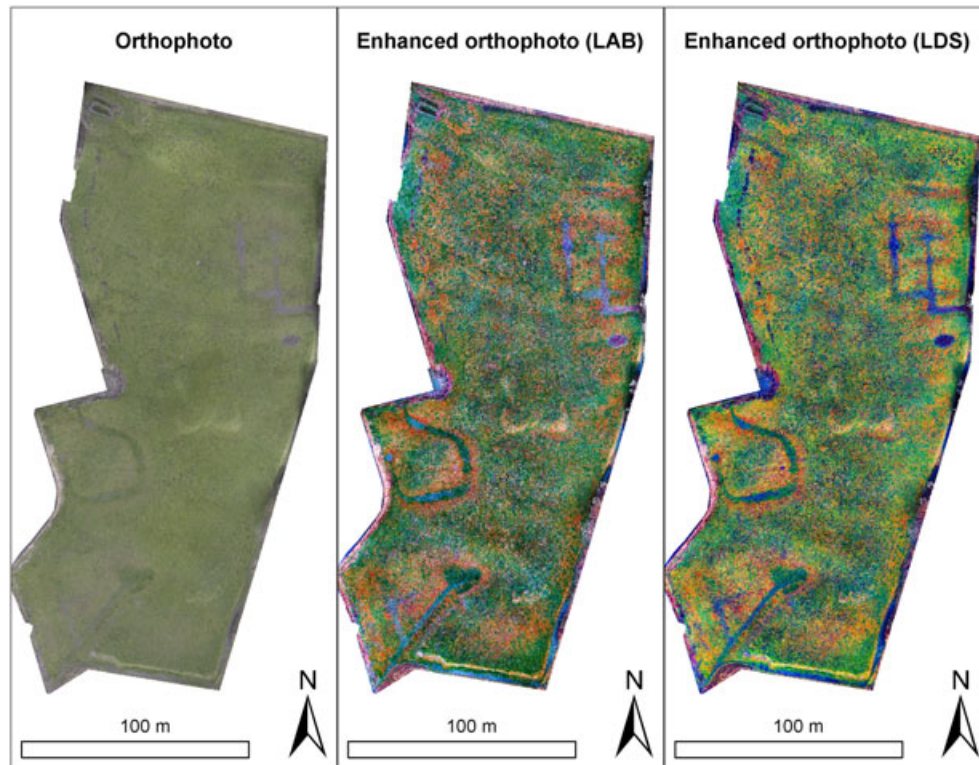


Figure 4. The orthophoto generated through image-based 3D reconstruction of the UAV survey imagery (left) and two decolouration stretched derivatives.

models, i.e. the 1986 topographic survey and the 2003 LiDAR survey (Figure 2). This is no surprise when we compare the raw data for each source, i.e. 2000 topographic measurements for the 1986 survey, 18,000 points for the 2003 LiDAR survey and a dense point cloud of more than 50 million points derived from the UAV imagery.

Although large archaeological features were already recognized in the LiDAR data, the UAV data provided more insights and details in these structures (Figure 5). Application of the algorithms to produce an enhanced visualization of the topographic variability led to a sequence of derivatives each highlighting the topography in a different way (Figure 3). Smaller (or more shallow) topographic features (e.g. the moated site, the plot-delineation and the port related ditches) were best visualized through the local topographic algorithms, while larger features (e.g. the dike, the U-shaped platforms and the ravelin of the small fortress) became clearer through the sky-view factor or the principle component analysis of the hill-shaded images. Additionally, the (enhanced) orthophotos shed yet another light on the archaeological landscape with clear crop marks (e.g. the small fortress), soil marks (e.g. one ditch of the double ditched road and the molehills) and watermarks (e.g. the moated site, the

plot-delineation and the port related ditches) (Figure 4). Only by combining these different layers, do we come to the archaeological interpretations described later, and summarized in Figure 5.

Integrating the (enhanced) orthophoto(s) with the DSM and derivatives to conduct a thorough analysis of the archaeological landscape, resulted in the identification of new archaeological features and the formulation of new hypotheses regarding the use and function of the main archaeological features. Six main features are discerned and will be discussed (Figure 5): (i) a dike, (ii) a small fortress (or sconce), (iii) port related features, (iv) a moated site, (v) parallel ditches and (vi) plot-delineations.

The dike stretches from north to south, and is characterized by a steep western slope (Figures 3, 5). The levee was erected on the left bank of the Zwin tidal inlet and cartographic material identifies it as the 'Hoogstraat' (High Street). The most southern part of the dike, where it bends and heads in south-western direction, could now be identified, as it juts out more distinctly in several visualizations. Two U-shaped platforms attached to the western side of the dike might be related to habitation, which is attested in proto-cadastral documents. From the elevation data, it is clear that a sconce was erected on the most

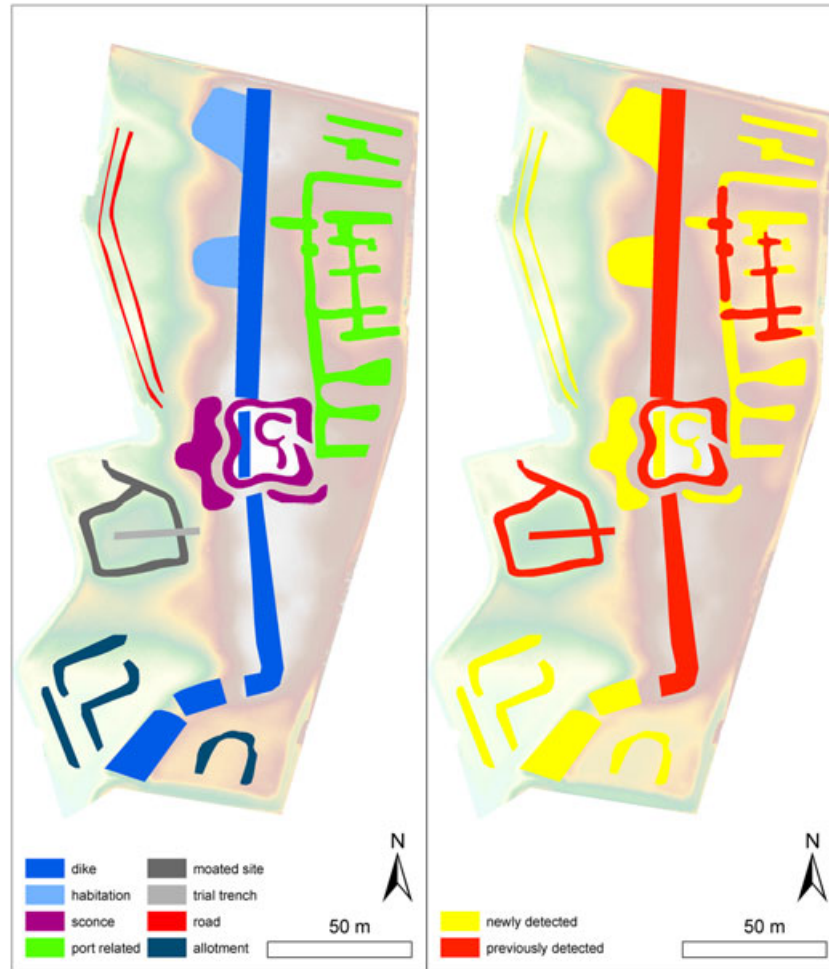


Figure 5. Interpretation of the topographic variability (left); with annotation of the newly detected features through the UAV survey data (right).

prominent location on top of the dike (Figures 5, 6). This rectangular fortification, measuring 25 m × 25 m, has its most prominent earthworks on its south and west sides. The northeast corner of the fort is least distinctive from its surroundings, probably due to erosion, but could clearly be delineated from the elevation data. An apparent gap in the eastern flank heads towards a circular, central feature which might be related with the internal organization of such a fortification. Adjacent to the western flank, a ravelin-like construction appears in the elevation data (e.g. slope and sky view factor). We can assume that the fortification was erected during the Eighty Year War, after the city had resigned its city right. This small fortress seems however to be unique in the abundant warfare-related archaeological record of the area (Poulain and De Clercq, 2015) and its precise military function and context needs further research.

A complex of potentially port-related linear features can be identified towards the northeast side of the field

(Figures 3, 4, 5), stretching into the former course of the tidal inlet and suggests a dockyard. From the new elevation data, these ditch-like features show a more interconnected structure consisting of east–west and north–south orientated patterns. The structure potentially extends in the southern direction, east of the sconce, where three east–west and one (potentially two) north–south orientated features can be identified. A moated site is located towards the west of the sconce, in a low-lying area at the foot of the dike (Figures 3, 4, 5). The ditches, platform and access of the moated site are clearly visible in the elevation data. Even the 1986 trial trench is clearly discernible. North of the moated site, adjacent to the small stream, a 4 m interval parallel double ditch appears for the first time (Figures 3, 4, 5). Written sources speak of the ‘Roostraat’ running in this direction. The map from 1695 however, situates this street at the other side of the stream. Finally, the analysis revealed subtle topographical features in the southern part of the field. These

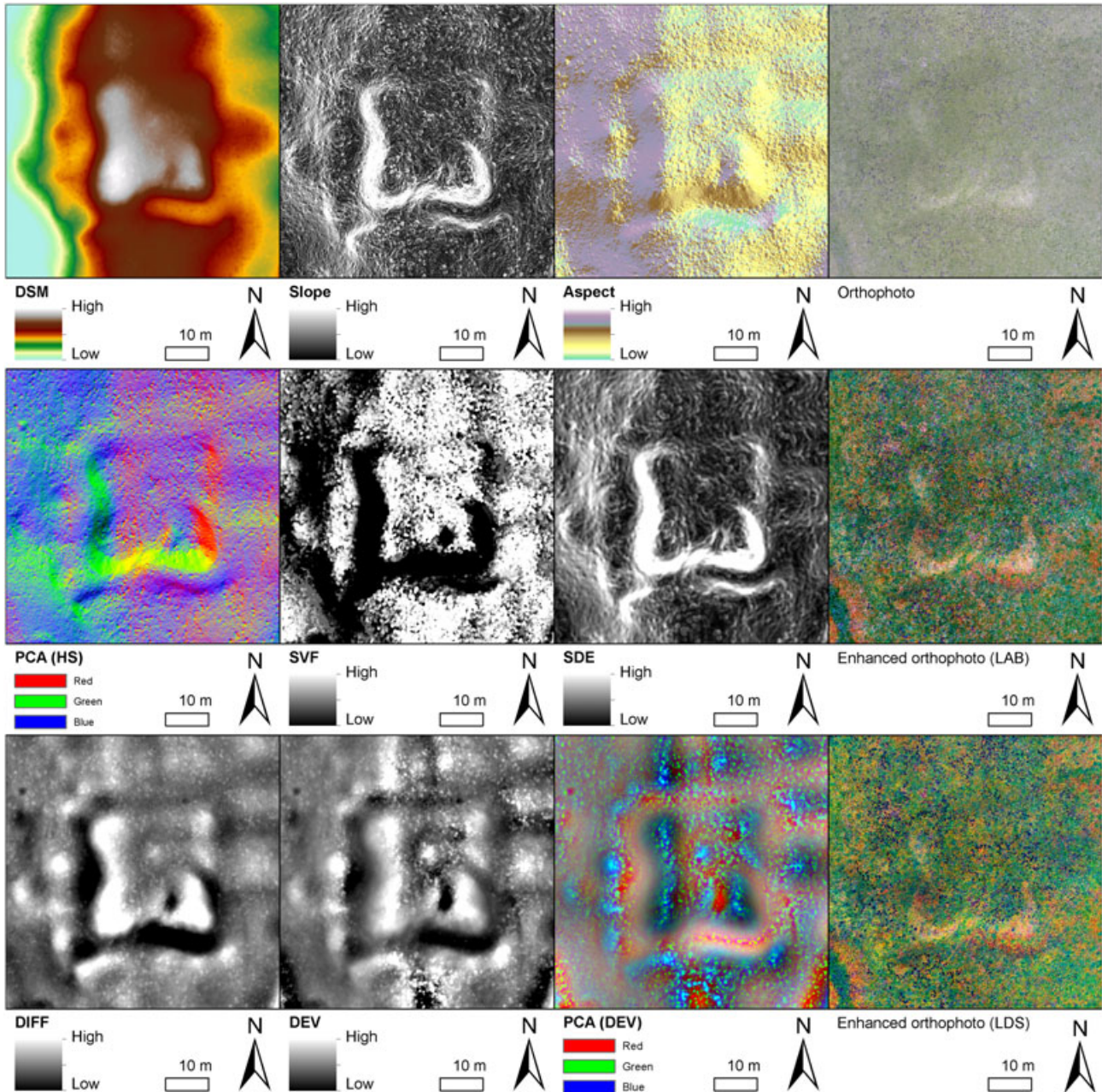


Figure 6. Detailed view of the sconce. DSM; slope (in percentage); slope orientation (aspect); principle component analysis of 16 hill-shaded images (PCA HS); sky-view factor (3 m search radius) (SVF); standard deviation of elevation (0.5 m search radius) (SDE); difference from mean elevation (5 m search radius) (DIFF); deviation from mean elevation (4 m search radius) (DEV); principle component analysis of 20 deviation from mean elevation images (search radii from 0.5 till 10 m, with 0.5 m interval) (PCA DEV); orthophoto and two decolleration stretched orthophotos.

features, most likely ditches, appear for the first time too, at both sides of the dike, and can probably be related to plot-delineations (Figures 3, 4, 5). This specific allotment was described in the proto-cadastral texts until 1481 but became merged into larger plots from 1517 onwards. Until now, these plots could not be identified in the field.

Although not of direct archaeological nature, but no less interesting was the detection of an enormous amount of molehills (approximately 5500) in the data. The molehills are visible in the topographic data, but became particularly clear as distinct clusters in the enhanced orthophotos (Figure 7). The data therefore provides an excellent record of the biological activity

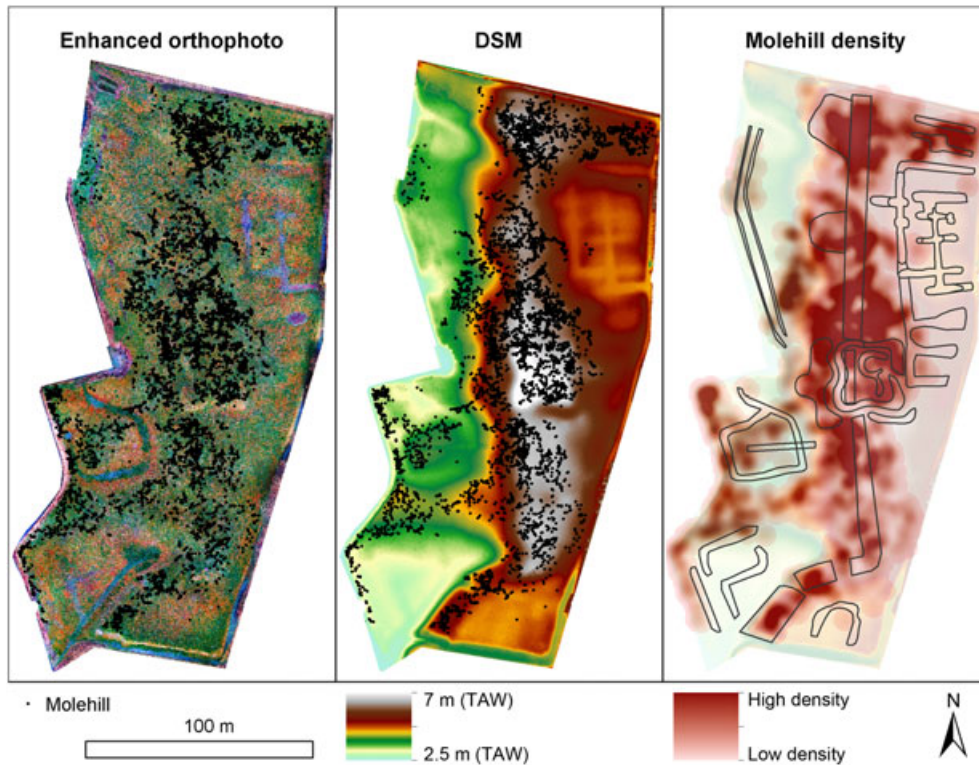


Figure 7. The molehills on the site, derived from the decoloration stretched orthophoto (left), plotted on the DSM (middle). A molehill density map indicates the intensity of bioturbation in relation to the archaeological features (right).

and its relationship with archaeological features at the site, while it also documents the extent of the bioturbation affecting the archaeological record.

Discussion

Our research aim was two-fold. First, we pursued a more detailed characterization and understanding of the microtopography of the landscape at Monnikerede, by means of an UAV survey, to achieve a better understanding of the buried archaeological landscape. Second, we assessed the potential of a consumer grade UAV solution for the image-based 3D reconstruction (and collection of high quality topographic data) of this complex Medieval landscape. Our results suggest that a consumer grade UAV solution can indeed be an excellent tool in archaeological prospection, allowing the generation of a highly detailed and accurate 3D model of the terrain. The elevation data that could be derived from the 3D model allowed a detailed topographic analysis of the complex archaeological landscape, leading to the detection of new archaeological features and new insights in the layout of this well-preserved Medieval landscape.

The UAV survey resulted in a highly detailed and accurate topographic model of the site. When compared with the first topographic survey (1986) and the first generation LiDAR (2003), the level of detail is proportionally higher. With this result, this low-cost survey can, without doubt, compete with the more expensive high-end solutions (e.g. Bendig *et al.*, 2013; Immerzeel *et al.*, 2014; second generation LiDAR). With more detail in the topographic model, the amount of information that could be derived from it and the gain of knowledge are significant. While the large archaeological features were already detected in and known from the LiDAR data and previous research, the high resolution (2.88 cm cell size) DSM allowed the detection and identification of microtopographic (archaeological) features in the landscape. Moreover, each of the applied visualization algorithms shed a different light on the topographic variability, each highlighting diverse aspects of the buried archaeological landscape. Only a combination of these tools led to a more global picture of the archaeology. As opposed to a LiDAR survey, the image-based 3D reconstruction captures textures, providing information about the texture, colour and appearance of the archaeological landscape. This means that, beside the topographic data, also archaeological marks in the vegetation (crop-, soil- and

shadowmarks), biological activity (e.g. mole activity) and land use (e.g. agriculture) are documented. In our case, five of the six main archaeological features are (partly) visible as crop marks, soil marks or watermarks in the imagery, providing an additional tool – which is unavailable through a LiDAR survey – for the interpretation of the topographic (and archaeological) variability. The enormous amount and clustering of molehills visible in the imagery provides an indication of the probable presence of archaeological contexts rich in organic matter as well as to the extent of bioturbation at the site.

The costs at which this high resolution data can be collected are relatively low – a consumer-grade UAV setup – making the method very beneficial to be implemented in archaeological survey, and particularly relevant for open areas where no (second generation) LiDAR is available. The combination of detailed topographic data with photorealistic (or enhanced) texture information makes the image-based 3D reconstruction a tool for research management and an excellent starting point for future research planning. In our case, the UAV survey precedes a geophysical electromagnetic induction (EMI) survey, and the results of both UAV survey and EMI survey will be integrated to develop a test pitting and augering survey strategy, to evaluate, identify and date the archaeological features. A map of the molehills, derived from the orthophoto, was used in aid of a field survey. The integration of different survey and evaluation techniques, starting from the detailed topographic image, will further develop our understanding of this Medieval landscape. In the longer run, the image-based 3D reconstruction is a document of historical interest. It captures and represents the site at a certain moment in its history, but it also helps to unravel various depositional processes that have led to the construction of the topography of the site as it reveals itself today. Natural processes, including erosion and biological activity (e.g. mole-activity) and cultural processes, including agriculture (e.g. cattle-trampling) and infrastructure (e.g. the sixteenth and nineteenth century canals), but also past archaeological research (e.g. trial trench 1986) are indeed continuously modifying the microtopography of this landscape.

Conclusion

Our research shows that even with a consumer grade UAV solution, we were able to conduct an aerial survey with image collection suitable for an accurate image-based 3D reconstruction of the landscape. The

high resolution topographic data that can be derived from these 3D models allows detailed analysis of the layout of an archaeological landscape. The texture present in the 3D models allows the detection of topographical features of archaeological nature. It shows that a consumer-grade UAV can be an integral part of the archaeologist's (survey) toolkit, and that the methodology will particularly be beneficial for (open) landscapes where no (second generation) LiDAR data is available. It provides an excellent record of an archaeological landscape or site, at a certain point in its history, with value for heritage management purposes aiming at the preservation and future monitoring of the site.

Acknowledgements

The government agency for Innovation by Science and Technology (IWT) is thanked for its financial support to the project 'Archaeology 3D: Towards a time-efficient and cost-effective recording of the archaeological heritage' (IWT-135118). The renewed archaeological research at Monnikerede is part of the Research Foundation Flanders (FWO)-funded project 'Medieval Bruges and its outer ports. A landscape-archaeological contribution to the Zwin debate' (3G004013). The authors appreciate the two anonymous referees of *Archaeological Prospection* for their helpful and useful comments and suggestions on an earlier version of this paper.

References

- AgiSoft LLC. 2015. Agisoft PhotoScan. *Professional Edition, Version 1.1.1*. <http://www.agisoft.com/> (accessed 19 February 2016).
- AGIV. 2003. Digitaal Hoogtemodel Vlaanderen. *Nieuwsbrief GIS-Vlaanderen* 16: 3–21.
- AGIV. 2008. Orthofoto's, middenschalig, kleur, provincie West-Vlaanderen, opname 2008. Agentschap voor Geografische Informatie Vlaanderen: Gent.
- Bendig J, Bolten A, Bareth G. 2013. UAV-based imaging for multi-temporal, very high resolution crop surface models to monitor crop growth variability. *Photogrammetrie – Fernerkundung – Geoinformation* 2013 (6): 551–562. DOI:10.1127/1432-8364/2013/0200.
- Bourgeois J, Roovers I, Meganck M, Semey J, Pelegrin R, Lodewijckx M. 2002. Flemish aerial archaeology in the last 20 years: past and future perspectives. In *Aerial archaeology. Developing Future Practice*, Bewley RH, Raczkowski W (eds), NATO Science Series. IOS Press: Amsterdam; 76–83.
- Caldwell D, Botzojorns U. 2014. An historic sign, possible Mesolithic menhir, DStretch, and problems in dating rock art to the Sauveterrian in the Massif de Fontainebleau. *Journal of Archaeological Science* 42: 140–151. DOI:10.1016/j.jas.2013.09.023.

- Cerrillo-Cuenca E, Sepúlveda M. 2015. An assessment of methods for the digital enhancement of rock paintings: the rock art from the precordillera of Arica (Chile) as a case study. *Journal of Archaeological Science* **55**: 197–208. DOI:10.1016/j.jas.2015.01.006.
- Chiabrando F, Nex F, Piatti D, Rinaudo F. 2011. UAV and RPV systems for photogrammetric surveys in archaeological areas: two tests in the Piedmont region (Italy). *Journal of Archaeological Science* **38**(3): 697–710. DOI:10.1016/j.jas.2010.10.022.
- Colomina I, Molina P. 2014. Unmanned aerial systems for photogrammetry and remote sensing: a review. *ISPRS Journal of Photogrammetry and Remote Sensing* **92**: 79–97. DOI:10.1016/j.isprsjprs.2014.02.013.
- De Reu J, Bourgeois J, Bats M, et al. 2013a. Application of the topographic position index to heterogeneous landscapes. *Geomorphology* **186**: 39–49. DOI:10.1016/j.geomorph.2012.12.015.
- De Reu J, De Smedt P, Herremans D, Van Meirvenne M, Laloo P, De Clercq W. 2014. On introducing an image-based 3D reconstruction method in archaeological excavation practice. *Journal of Archaeological Science* **41**: 251–262. DOI:10.1016/j.jas.2013.08.020.
- De Reu J, Plets G, Verhoeven G, et al. 2013b. Towards a three-dimensional cost-effective registration of the archaeological heritage. *Journal of Archaeological Science* **40**(2): 1108–1121. DOI:10.1016/j.jas.2012.08.040.
- De Smet A. 1937. L'origine des ports de Zwin. Damme, Mude, Monikerede, Hoeke et Sluis. In *Etudes d'histoire dédiées à la mémoire de Henri Pirenne par ses anciens élèves*. Nouvelle société d'éditions: Brussels; 125–141.
- Devereux BJ, Amable GS, Crow P. 2008. Visualisation of LiDAR terrain models for archaeological feature detection. *Antiquity* **82**(316): 470–479. DOI:10.1017/S0003598X00096952.
- Doneus M, Verhoeven G, Fera M, Briese C, Kucera M, Neubauer W. 2011. From deposit to point cloud – a study of low-cost computer vision approaches for the straightforward documentation of archaeological excavations. In *XXIIIrd International CIPA Symposium, Prague, 12–16 September 2011*. Geoinformatics, Čepěk A (ed). Faculty of Civil Engineering, Czech Technical University: Prague; 81–88.
- Eisenbeiss H, Sauerbier M. 2011. Investigation of UAV systems and flight modes for photogrammetric applications. *The Photogrammetric Record* **26**(136): 400–421. DOI:10.1111/j.1477-9730.2011.00657.x.
- Gallant JC, Wilson JP. 2000. Primary topographic attributes. In *Terrain Analysis: Principles and Applications*, Wilson JP, Gallant JC (eds). Wiley: New York; 51–85.
- Gilliodts-Van Severen L. 1891. Coutumes des petites villes et seigneuries enclavées 3. Gobbaerts: Brussels.
- Harman J. 2014. DStretch (plugin to ImageJ). <http://www.dstretch.com/> (accessed 19 February 2016).
- Hillewaert B. 1986. La petite ville de Monnikerede: analyse duo relief et étude microtopographique. *Scholae Archaeologicae*, 4. Seminarie voor Archeologie, Rijksuniversiteit Gent: Gent.
- Immerzeel WW, Kraaijenbrink PDA, Shea JM, et al. 2014. High-resolution monitoring of Himalayan glacier dynamics using unmanned aerial vehicles. *Remote Sensing of Environment* **150**: 93–103. DOI:10.1016/j.rse.2014.04.025.
- Janssen HQ. 1854. Monnikereede. *Cassandra* 73–95.
- Kokalj Z, Zaksek K, Ostir K. 2011. Application of sky-view factor for the visualisation of historic landscape features in lidar-derived relief models. *Antiquity* **85**(327): 263–273. DOI:10.1017/S0003598X00067594.
- Koutsoudis A, Vidmar B, Ioannakis G, Arnaoutoglou F, Pavlidis G, Chamzas C. 2014. Multi-image 3D reconstruction data evaluation. *Journal of Cultural Heritage* **15**(1): 73–79. DOI:10.1016/j.culher.2012.12.003.
- Lucieer A, de Jong S, Turner D. 2013. Mapping landslide displacements using Structure from Motion (SfM) and image correlation of multi-temporal UAV photography. *Progress in Physical Geography* **38**(1): 97–116. DOI:10.1177/0309133313515293.
- Nex F, Remondino F. 2014. UAV for 3D mapping applications: a review. *Applied Geomatics* **6**(1): 1–15. DOI:10.1007/s12518-013-0120-x.
- Ortiz J, Gil ML, Martínez S, Rego T, Meijide G. 2013. Three-dimensional modelling of archaeological sites using close-range automatic correlation photogrammetry and low-altitude imagery. *Archaeological Prospection* **20**(3): 205–217. DOI:10.1002/arp.1457.
- Poulain M, De Clercq W. 2015. Exploring an archaeology of the Dutch War of Independence in Flanders, Belgium. *International Journal of Historical Archaeology* **19**(3): 623–646. DOI:10.1007/s10761-015-0301-x.
- Ryckaert M, Vandewalle A. 1982. De strijd voor het behoud van het Zwin. In *Brugge en de zee: van Bryggia tot Zeebrugge*. Mercatorfonds: Antwerpen; 52–70.
- Sosson J. 1993. Les petites villes du Zwin (XIVe – XVe siècles) des espaces urbains inviables. In *Commerce, finances et société (XIe – XVIe siècles)*. Recueil de travaux d'histoire médiévale offert à M. le Professeur Henri Dubois, Contamine P, Dutour T, Schnerb B (eds). Presses de l'université de Paris-Sorbonne: Paris; 171–184.
- Torres-Sánchez J, López-Granados F, De Castro AI, Peña-Barragán JM. 2013. Configuration and specifications of an unmanned aerial vehicle (UAV) for early site specific weed management. *PLoS One* **8**(3e58210):. DOI:10.1371/journal.pone.0058210.
- Verhoeven G. 2011. Taking computer vision aloft – archaeological three-dimensional reconstructions from aerial photographs with photostan. *Archaeological Prospection* **18**(1): 67–73. DOI:10.1002/arp.399.
- Verhoeven G, Doneus M, Briese C, Vermeulen F. 2012. Mapping by matching: a computer vision-based approach to fast and accurate georeferencing of archaeological aerial photographs. *Journal of Archaeological Science* **39**(7): 2060–2070. DOI:10.1016/j.jas.2012.02.022.
- Watts AC, Ambrosia VG, Hinkley EA. 2012. Unmanned aircraft systems in remote sensing and scientific research: classification and considerations of use. *Remote Sensing* **4**(6): 1671–1692. DOI:10.3390/rs4061671.
- Werbrouck I, Antrop M, Van Eetvelde V, et al. 2011. Digital elevation model generation for historical landscape analysis based on LiDAR data, a case study in Flanders (Belgium). *Expert Systems with Applications* **38**(7): 8178–8185. DOI:10.1016/j.eswa.2010.12.162.
- Whitehead K, Hugenholtz CH. 2014. Remote sensing of the environment with small unmanned aircraft systems (UASs), part 1: a review of progress and challenges.

- Journal of Unmanned Vehicle Systems* 2(3): 69–85. DOI:10.1139/juvs-2014-0006.
- Whitehead K, Hugenholtz CH, Myshak S, et al. 2014. Remote sensing of the environment with small unmanned aircraft systems (UASs), part 2: scientific and commercial applications. *Journal of Unmanned Vehicle Systems* 2(3): 86–102. DOI:10.1139/juvs-2014-0007.
- Zakšek K, Oštir K, Kokalj Ž. 2011. Sky-view factor as a relief visualization technique. *Remote Sensing* 3(2): 398–415. DOI:10.3390/rs3020398.